DE GRUYTER OPEN

Acta Palaeobotanica 55(2): 183–207, 2015
DOI: 10.1515/acpa-2015-0010

Palynostratigraphy, palynofacies and depositional environment of a lignite-bearing succession at Surkha Mine, Cambay Basin, north-western India

PRIYANKA MONGA[1], MADHAV KUMAR[1], VANDANA PRASAD[1] and YOGESH JOSHI[2]

[1] Birbal Sahni Institute of Palaeobotany, 53, University Road, Lucknow 226007, India;
e-mail: priyankamongapu@gmail.com; madhavbsip@gmail.com; prasad.van@gmail.com
[2] Department of Botany, S. S. J. Campus, Almora, India; e-mail: dryogeshcalo@gmail.com

Received 1 April 2015; accepted for publication 22 September 2015

ABSTRACT. The paper reports palynology and palynofacies studies of lignite-bearing sediments exposed in an opencast mine succession at Surkha, Bhavnagar District, in the coastal region of Gujarat, India. The study examined the relationships between the palynoflora, sedimentary organic matter and environment at the time of deposition of lignite and associated sediments. Based on dinoflagellate cyst biostratigraphy, the sedimentary succession is dated as early Eocene (Ypresian). Palynofacies studies helped reveal the palaeoenvironmental fluctuations. The dominance of angiosperm pollen grains, freshwater algae, microthyraceous fungi and a large share of land debris in the lower part of the succession suggests a freshwater swamp environment of deposition for the basal lignite facies. Two cenozones – *Matanomadiasulcites maximus* and *Lakiapollis ovatus* – were identified in the lower lignite facies, determined from the dominance of these pollen grains in the palynological assemblages. The presence of angiosperm pollen grains and pteridophyte spores in the carbonaceous shale horizon above the lignite facies indicates a change in the depositional regime from freshwater swamp to lagoonal. This was identified as the *Arecipites wodehousei* cenozone due to its numerical abundance in the assemblage. Dinoflagellate cyst abundance and diversity, and microforaminiferal test linings along with well-sorted terrestrial debris in the mudstone in the upper part of the succession suggest a more open marine estuarine type of depositional environment. The *Homotryblium* complex along with *Cordospheridium fibrospinosum*, *Kenleyia* sp., and *Thalassiphora pelagica* dinoflagellate cysts are the main representatives of this zone, determined as the *Homotryblium tenuispinosum* cenozone. The changing depositional settings (freshwater swamp–lagoonal–estuarine) along the vertical succession indicate a marine transgression in this region. Results from palynological studies of early Palaeogene successions of the Cambay and Kutch basins correlate well with the present findings.

KEYWORDS: palynostratigraphy, palynofacies, palaeoenvironment, Early Eocene, western India

INTRODUCTION

The early Palaeogene greenhouse period has attracted much attention over the last decades, as it provides a natural example of vegetation response to global warming (Morley 2000, Zachos et al. 2001, Wing et al. 2005). The palaeoclimatic and palaeoenvironmental fluctuations of this period have been studied far and wide across the globe. Extensive lignite and associated deposits were formed under fluvial and marine influences in western India during early Palaeogene post-Deccan Traps eruptions in the Cambay Basin, Gujarat, India (Samant & Mohabey 2005, 2014, Sahni 2006). Various factors such as distance from the marine source, local topography, vegetation pattern, and variation in clastic supply from the land played a major role in shaping these paralic lignite deposits. Here we report the first study of palaeoenvironmental fluctuations assessed from a sedimentary succession

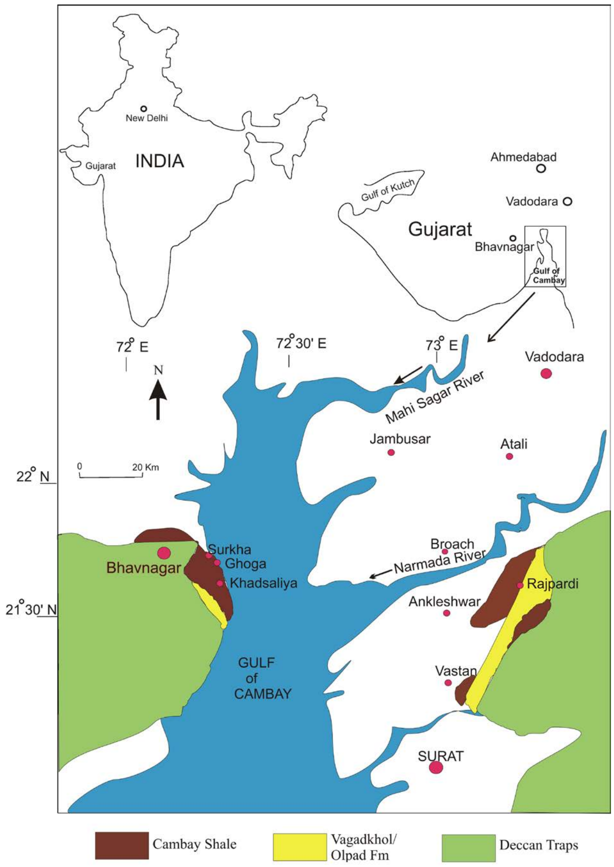

Fig. 1. Geological map and location of the study area

exposed at the Surkha lignite mine (21°26′43″–21°42′00″N; 72°07′30″–72°16′30″E) in Ghogha Talukas, Bhavnagar District, Gujarat (Cambay Basin) (Fig. 1), based on palynological and palynofacies parameters. The succession consists of rhythmic deposits of lignite, carbonaceous shale, mudstone, and carbonate muddy matrix (lithology in Fig. 2), and is considered equivalent to the Cambay Shale Formation of Cambay Basin. The organic-rich facies of Cambay Shale Formation have been identified as the major source rock unit for hydrocarbon generation in the Cambay Basin (Mohan 1995, Banerjee et al. 2000, Bhandari & Raju 2000, Sivan et al. 2008, Madhavi et al. 2009). The sediments are exceptional material for studying tropical floral elements and sedimentary organic matter content, their succession, the variability of the various lithotypes, and depositional environments during the early Eocene.

Palynology is an excellent tool for interpreting palaeoclimatic variations on the basis of the distribution of terrestrial and marine palynofossils in a sedimentary horizon (Traverse 1988, Larsson et al. 2006), while palynofacies analysis deals with the palaeoenvironmental and biological characteristics of organic facies (Tyson 1995, Batten 1996). Our palynological analysis of the Surkha lignite succession revealed characteristic palynomorphs originating from marine and non-marine sources. The terrestrial palynomorphs present in the sediments are spores, pollen grains, and fungal fruiting bodies; marine palynomorphs are represented by dinoflagellate cysts. Earlier palynological studies investigated the Rajpardi and Vastan lignite mines (Kar & Bhattacharya 1992, Kumar 1996, Samant & Phadtare 1997, Garg et al. 2008, Prasad et al. 2009, Tripathi & Srivastava 2012, Prasad et al. 2013, Rao et al. 2013), and there are also palaeontological studies (Rana et al. 2004, Bajpai et al. 2005a,b, Nagori et al. 2013). The present paper reports a quantitative and qualitative study of terrestrial and marine palynomorphs aimed at disclosing the vegetational pattern and palaeoenvironmental conditions at the time of deposition of the Surkha lignite mine succession, and understanding past tropical ecosystems.

GEOLOGICAL SETTING

The Cambay Basin is an intra-cratonic, north-south-trending rift sag Tertiary basin, in the western onshore part of India (Banerjee et al. 2000). The basin is elliptical in outline, bounded by the Saurashtra uplift in the west, the hills of the Aravali range in the east, and the Kutch Basin in the north. Deposition of sediments in the basin started during the Late Mesozoic with the development of major tensional faults following widespread extrusion of the Deccan Traps basalt (Agrawal 1986, Dayal et al. 2013). The Deccan Traps cover the major portion of the Saurashtra peninsula and form the basement for the development of Tertiary and Quaternary sediments in the basin. The Tertiary sediments comprise grey wacks, dark grey to black grey shale, lignite, silts, fine to medium-grained sands, and grey reddish brown clays (Bhandari & Choudhary 1975).

Stratigraphically the rock and sedimentary sequences of the basin are categorised into eight formations (Vagadkhol, Cambay Shale, Ankleshwar, Tadkeshwar, Babaguru, Kand, Jhagadia, Narmada), with the Deccan Traps forming the basement overlain by the Cambay Shale Formation (Agrawal 1986). The Cenozoic sediments are ca 200–300 m thick and contain various types of plant microfossils (e.g. spores, pollen grains, dinoflagellates, sedimentary organic matter) along with megafloral and faunal remains. Table 1 gives the general stratigraphic succession of the Cambay Basin (after Agarwal 1986).

MATERIAL AND METHODS

PALYNOFLORAL AND PALYNOFACIES ANALYSES

The study is based on the palynoflora and sedimentary organic matter (palynofacies) obtained through chemical processing of sediment samples collected from the lignite and associated sequences. Standard techniques were followed for extraction of palynomorphs and organic particles (Brown 1960, Batten & Morrison 1983). Sixty samples of argillaceous lithotypes (e.g. lignite, carbonaceous shale, greenish/grey clay, mudstone, siliceous clay) were collected from measured parts of a freshly exposed section. The palynological samples were collected from a 30–60 cm interval of lignite and a 20–25 cm interval of carbonaceous shale and muddy matrices. For palynofloral analysis, crushed carbonaceous shale and clay samples were kept in dilute hydrochloric acid for 18 h, followed by treatment with 40% hydrofluoric acid for 3–4 days; after decantation of the acidic water, the digested material was sieved through 20-micron mesh. The lignite samples were kept in concentrated nitric acid for 3–4 days, washed, and then treated with 3–4% solution of potassium hydroxide for 2–4 min, followed by decantation of the acidic water. To recover sedimentary organic matter, the samples were treated with concentrated hydrochloric acid for 12 h, washed 2–3 times with water, and then kept in 40% hydrofluoric acid for 3–4 days, followed by treatment with aqueous ammonia solution for 2–3 min. Macerated residues containing palynoassemblages and sedimentary organic matter were smeared by mixing with polyvinyl alcohol solution on cover slips, dried in an oven for ca 30 min., and mounted on slides with Canada balsam. The frequency of palynomorphs and types of sedimentary organic matter were determined in each sample by counting 200 palynotaxa and 500 different types of sedimentary organic matter. Recovered palynomorphs were classified following the system of classification proposed by Potonié and Kremp (1955, 1956). The classification of sedimentary organic matter (palynofacies) follows Masran & Pocock (1981), Pocock et al. (1988), and Batten (1996).

FLUORESCENCE MICROSCOPY

UV fluorescence microscopy was used to characterise the various types of sedimentary organic matter. Microscope slides were observed under 530–600 nm UV blue light after excitation for 2–5 min (van Gijzel 1982) to distinguish different organic constituents, which reflect the preservation state and biological origin of the components (Staplin 1969, Tyson 1995).

RESULTS AND DISCUSSION

PALYNOFLORAL AGE CONTROL AND COMPARISON WITH OTHER CONTEMPORANEOUS DEPOSITS OF NORTH-WESTERN INDIA

The age of the sediments of the Cambay Shale exposed at the Surkha lignite mine was determined on the basis of the presence of dinoflagellate cysts and angiosperm pollen grains.

Table 1. Generalised stratigraphy succession of the Cambay Basin

Age			Formation and Thickness	Lithology
Cenozoic	Quaternary	Holocene	Narmada Fm.	Sandstone, silt, clay, gravel
			Unconformity	
		Lower Pliocene	Jhagadia Fm. (200 m)	Sandstone, gritstone, conglomerate, breccia, clay, silt
			Unconformity	
		Miocene	Kand Fm. (200–400 m)	Conglomerate, fossil, limestone, calcareous sandstone, gravelly clay
			Unconformity	
			Babaguru Fm. (200–300 m)	Conglomerate, agate, sandstone, clays, cherry red, highly ferruginous
	Tertiary		Unconformity	
		Oligocene	Tadkeshwar Fm. (125–346 m)	Unconformity
			Unconformity	
		Eocene	Ankleshwar Fm. (603 m)	Limestone, fossils, breccia, marls
			Unconformity	
			Cambay Shale (+1500 m)	Grey to dark grey thinly bedded shales
			Unconformity	Conglomerate, grit, sandstone, variegated clays, sandstone
		Palaeocene	Vagadkhol Fm (+50 m)	
			Unconformity	
Mesozoic		Cretaceous	Deccan Trap	Basalts, sometimes amyadaloidal and trachytic

Though dinoflagellates are present in selected levels and have wide vertical ranges of occurrence, a few dinoflagellate cyst marker taxa (e.g. *Homotryblium tenuispinosum*, *H. abbreviatum*, *Cordosphaeridium fibrospinosum*, *Kenleyia* sp.) place the *Homotryblium tenuispinosum* FAD in the late Thanetian, and the *H. abbreviatum* FAD in the middle Ypresian (Powell 1992, Williams et al. 2004), suggesting early Eocene age for the succession. *Thalassiphora pelagica* dinoflagellate cysts present in the middle part of the succession show stratigraphy in the Ypresian (56.8–48.6 mya) of the Northern Hemisphere (Williams et al. 1993, Toricelli et al. 2006). *Homotryblium tenuispinosum* is also recorded from the Nammal Formation (early Eocene), the Salt Range of Pakistan (Edwards 2007), and the Polosatya Formation of Kazakhstan (Iakovleva et al. 2001). *Thalassiphora pelagica* is present in the early Eocene of the Peri-Tethys of Kazakhstan (King et al. 2013) and from north-west Borneo (Besems 1992). *Kenleyia* sp. is characteristic of the basal Eocene (dinocyst zone NZE1a) of the Tawanui section of New Zealand (Crouch et al. 2003) and is also present in the lower part of the middle succession. The first appearance datum (FAD) of *Cordosphaeridium fibrospinosum* is from the middle Ypresian of Brecklesham beds of Whitecliff Bay (Bujak et al. 1980, Powell 1992). *Cordosphaeridium fibrospinosum* is also recorded from Early Eocene sediments of New Zealand (Wilson 1988). The present dinoflagellate cyst assemblage correlates well with the dinocyst assemblage of the middle part of the Vastan lignite mine succession, Cambay Basin (Garg et al. 2008), and the lower horizon of the Naredi Formation, Kutch (Garg et al. 2011).

Palynological studies of the Cambay Shale Formation have been done in material from the Rajpardi lignite (Kar & Bhattacharya 1992, Kumar 1996, Samant & Phadtare 1997), and from the Vastan lignite (Mandal & Guleria 2006, Tripathi & Srivastava 2012, Rao et al. 2013). Some significant spores and pollen grains common to the present assemblage and that from Rajpardi are *Cyathiditis australis*, *Lygodiumsporites lakiensis*, *Dandotiaspora telonata*, *D. plicata*, *Arecipites* sp., *Longapertites vaneendenburgi*, *Palmaepollenites kutchensis*, *P. eocenicus*, *Palmidites plicatus*, *Arengapollenites* spp., *Spinizonocolpites echinatus*, *Clavaperiporites heteroclavatus*, *Lakiapollis ovatus*, *Matanomadhiasulcites maximus*, *Dermatobrevicolporites dermatus*, and *Rhoipites kutchensis*. The Surkha lignite has spores and pollen grains in common with taxa recovered from the Vastan lignite: *Cyathidites australis*, *Lygodiumsporites lakiensis*, *L. pachyexinus*, *Dandotiaspora telonata*, *Arecipites bellus*, *Spinizonocolpites echinatus*, *Matanomadhiasulcites maximus*, *Lakiapollis ovatus*, *Dermatobrevicolporites dermatus*, *Rhoipites kutchensis*, *Clavaperiporites clavatus*, and *Retipollenites confusus*. The palynofloras from the Naredi Formation, Kutch, Gujarat (Venkatachala & Kar 1969, Kar 1985) are rich and have many forms also found in the present study (e.g. *Lygodiumsporites lakiensis*, *Arecipites bellus*, *Spinizonocolpites echinatus*, *Lakiapollis ovatus*). Thus the biostratigraphic study clearly points to early Eocene age for the Surkha succession.

PALYNOSTRATIGRAPHY

The sediments of the Cambay Shale Formation at the Surkha lignite mine contain a large amount of diverse and well preserved plant-derived phytoclasts in various lithotypes. The basal and middle parts of the section show dominance of angiosperm pollen grains with abundant fungal fruiting bodies, while the upper part contains abundant dinoflagellate cysts with pteridophyte spores. The stratigraphic and ecologically significant palynotaxa were quantitatively assessed for delineation of the palynostratigraphic zonation. The different palynozones also demarcate the first and last appearance of the palynomorphs, their maximum abundance, range in the vertical column, and restricted occurrences of many palynotaxa. The temporal distribution pattern of fossil spores, pollen grains, and dinoflagellate cysts recovered from individual samples indicates four cenozones (*Matanomadhiasulcites maximus*, *Lakiapollis ovatus*, *Arecipites wodehousei*, *Homotryblium tenuispinosum*) in ascending stratigraphic order (Fig. 2).

***Matanomadhiasulcites maximus* cenozone**

Lithology. The vertical range of the cenozone is limited to basal lignite (0.5 m thick) and overlying carbonaceous shale (0.5 m thick).

Position. Samples 5–8.

Palynoassemblage. This palynozone is marked by the significant dominance of

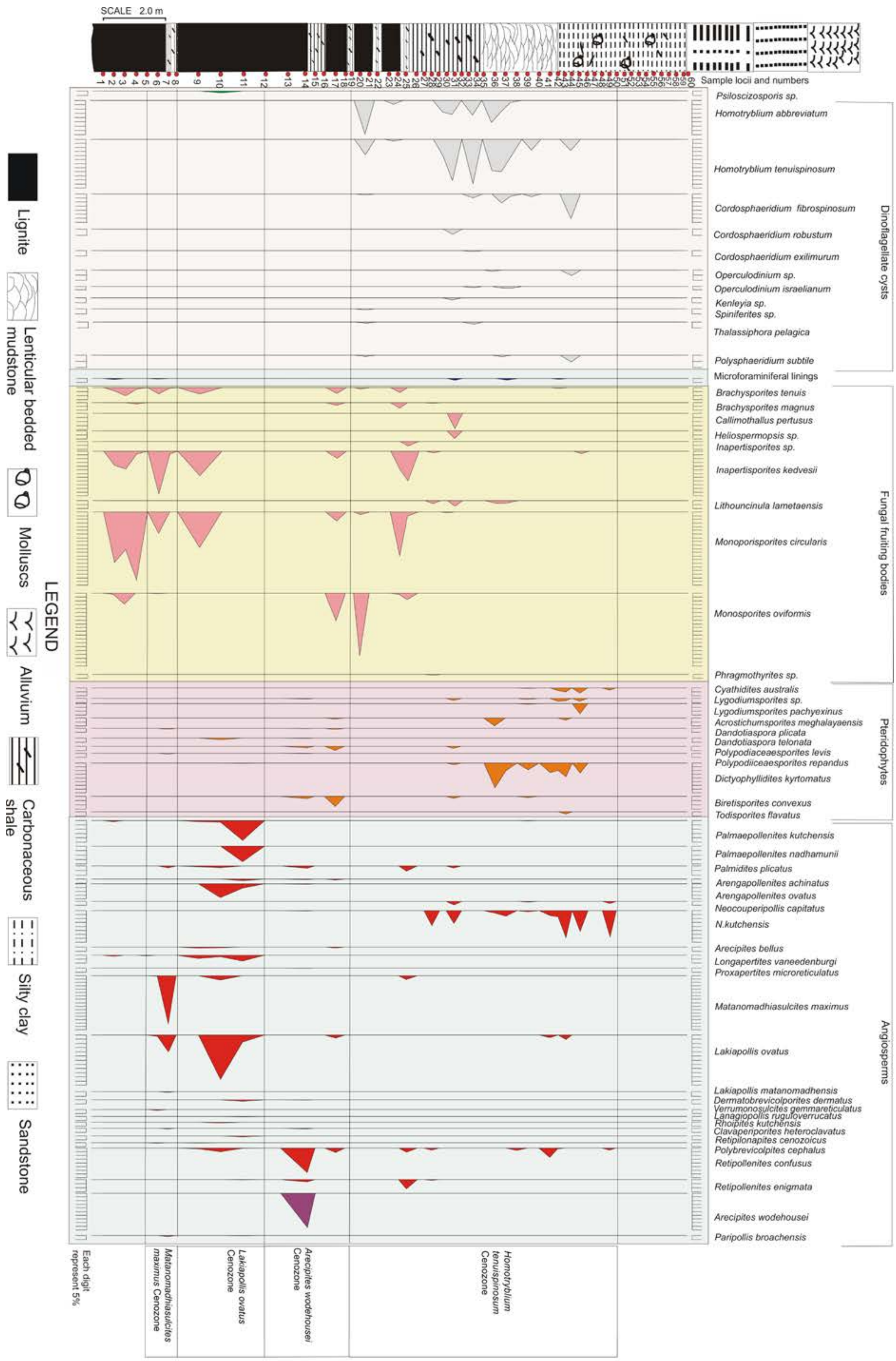

Fig. 2. Palynostratigraphic zonation of Surkha lignite mine section

Matanomadhiasulcites maximus (70%) in sample 7, which diminishes in the upper strata. In descending order of abundance, the other material comprises pollen grains of *Lakiapollis ovatus*, *Palmidites plicatus*, tetrads of *Paripollis broachensis*, *Verrumonosulcites gemmareticulatus*, *Retipilonapites cenozoicus*, *Clavaperiporites heteroclavatus*, *Rhoipites kutchensis*, and *Lakiapollis matanomadhensis*, and spores of *Dandotiaspora plicata* and *Polypodiaceasporites levis*. The presence of pollen grains of *Lakiapollis matanomadhensis*, *Verrumonosulcites gemmareticulatus*, and *Clavaperiporites heteroclavatus* is restricted to this zone. The fungal fruiting bodies represented here are *Monoporisporites circularis*, *M. ovaliformis*, *Inapertisporites kedvesii*, *Brachysporites tenuis*, and *B. magnus*. *Botryococcus braunii* alga and microforaminiferal linings (1–2%) also appear in the assemblage.

Upper limit. The decline in pollen frequency of *Matanomadhiasulcites maximus*, *Lakiapollis ovatus*, and *Palmidites plicatus* mark the upper limit of this cenozone.

Remarks. The overall flora represents abundant pollen grains of *Matanomadhiasulcites maximus*, *Lakiapollis ovatus*, and *Palmidites plicatus*, with fungal fruiting bodies.

Lakiapollis ovatus cenozone

Lithology. The vertical range of this cenozone is confined to a 2.25 m thick lignite seam.

Position. Samples 9–12.

Palynoassemblage. The cenozone is marked by the highest frequency of *Lakiapollis ovatus* (50–60%), recorded in sample 10. In descending order of abundance, the important species recovered are *Palmaepollenites kutchensis*, *P. nadhamunii*, *Arengapollenites ovatus*, *Longapertites vaneedenburgi*, *Matanomadhiasulcites maximus*, *Retipollenites confusus*, *Arengapollenites achinatus*, *Palmidites plicatus*, *Arecipites bellus*, *Dermatobrevicolporites dermatus*, *Retipilonapites cenozoicus*, *Rhoipites kutchensis*, and *Lanagiopollis ruguloverrucatus*. The taxa showing their first and last appearance in this cenozone are *Palmaepollenites nadhamunii*, *Longapertites vaneedenburgi*, *Dermatobrevicolporites dermatus*, *Retipilonapites cenozoicus*, *Rhoipites kutchensis*, and *Lanagiopollis ruguloverrucatus*. Spores of *Dandotiaspora telonata* and fungal fruiting bodies of *Monoporisporites circularis*, *M. ovaliformis*, *Inapertisporites kedvesii*, *Inapertisporites* sp., and *Brachysporites tenuis*, along with freshwater algal spores of *Psiloschizosporis* sp., are also recorded in this cenozone.

Lower limit. The first appearance of pollen grains of *Palmaepollenites kutchensis*, *Palmidites plicatus*, *Arecipites bellus*, *Longapertites vaneedenburgi*, and *Retipollenites confusus* mark the lower limit of this cenozone.

Upper limit. The steep decline in pollen of *Palmaepollenites kutchensis*, *Palmidites plicatus*, *Arengapollenites ovatus*, and *Longapertites vaneedenburgi* marks the upper limit of this cenozone.

Remarks. The overall palynoflora of this cenozone is dominated by palms.

Arecipites wodehousei cenozone

Lithology. The cenozone occupies the upper part of the lignite seam and carbonaceous shale (2.0 m thick).

Position. Samples 13–18.

Palynoassemblage. The cenozone is named after the first appearance of *Arecipites wodehousei*, the abundance of which peaks in sample 14 (40%). The other recovered material consists of pollen grains of *Palmidites plicatus*, *Arengapollenites achinatus*, *Arecipites bellus*, *A. ovatus*, *Palmidites plicatus*, *Lakiapollis ovatus*, *Clavaperiporites heteroclavatus*, *Retipollenites confusus*, and *R. enigmata*, and pteridophyte spores of *Biretisporites convexus*, *Dandotiaspora telonata*, *D. plicata*, *Lygodiumsporites* sp., and *Acrostichumsporites meghalayaensis*. Pollen grains of *Retipollenites confusus*, *R. enigmata*, *Neocouperipollis kutchensis*, and *Palmidites plicatus* appear in strata overlying this cenozone. Fungal fruiting bodies of *Monoporisporites ovaliformis*, *M. circularis*, *Inapertisporites kedvesii*, *Calimothallus pertusus*, *Brachysporites tenuis*, and *B. magnus* were also recorded in this interval.

Lower limit. The lower limit is marked by the presence of pollen grains of *Arecipites wodehousei* and *Retipollenites enigmata*, and an increase in the frequency of pteridophyte spores.

Remarks. The palynoflora is distinguished by decreased abundance of palms and an increase in the frequency of pteridophyte spores.

Homotryblium tenuispinosum cenozone

Lithology. This cenozone spans the middle to the top of the section (9.0 m thick), comprising upper lignite and carbonaceous shale, mudstone, and carbonaceous muddy matrix.

Position. Samples 19–50.

Palynoassemblage. The cenozone is marked by the peak of the dinoflagellate cyst *Homotryblium tenuispinosum* (45%) in samples 30 and 34 of the middle and upper parts of the section. The overlying lenticular bedded mudstone and upper carbonaceous shale shows lower frequency of this species (25–10%). The other subdominant dinoflagellate cysts represented here are *Homotryblium abbreviatum*, *Cordosphaeridium fibrospinosum*, *C. robustum*, *C. exillimurum*, *Thalassiphora pelagica*, *Operculodinium israelianum*, *Operculodinium* sp., *Polysphaeridium subtile*, and *Spiniferites* sp., with some microforaminiferal linings (2–3%), along with angiosperm pollen grains of *Neocouperipollis kutchensis*, *N. capitatus*, *Matanomadhiasulcites maximus*, *Palmidites plicatus*, *Lakiapollis ovatus*, *Polybrevicolpites cephalus*, *Retipollenites enigmata*, and *R. confusus*. The pteridophyte spores recorded in this interval are *Dictyophyllidites kyrtomatus*, *Acrostichumsporites meghalayensis*, *Todisporites flavatus*, *Lygodiumsporites pachyexinus*, *Lygodiumsporites* sp., *Cyathidites australis*, *Polypodiaceaesporites levis*, and *Biretisporites convexus*. Fungal fruiting bodies of *Callimothallus pertusus*, *Monoporisporites circularis*, *M. oviformis*, *Lithouncinula lanetaensis*, *Heliospermopsis* sp., *Brachysporites magnus*, *B. tenuis*, and *Inapertisporites kedvesii* were also recovered, along with microforaminiferal linings.

Lower limit. The lower limit is marked by the first appearance of dinoflagellate cysts of *Homotryblium tenuispinosum* and *Homotryblium abbreviatum*, and pollen grains of *Neocouperipollis kutchensis* and *N. capitatus.*

Upper limit. An increase in *Neocouperipollis kutchenis* abundance and a decrease of *N. capitatus* and *Polybrevicolpites cephalus* pollen grains mark the upper limit of this cenozone.

Remarks. The overall flora is dominated by dinoflagellate cysts, with abundant pteridophyte spores. The overlying strata above this cenozone (samples 50–60) are devoid of any palynofloral assemblages.

PALYNOFLORA AND PALAEOVEGETATION

Our palynofloral analysis of the Surkha lignite mine section yielded a scenario of the palaeovegetation types and succession during the deposition of its various strata. The palynoflora is represented by pteridophytes (13 genera, 15 species), angiosperms (30 genera, 46 species), fungal fruiting bodies (12 genera, 12 species), dinoflagellate cysts (7 genera, 11 species), and microforaminiferal linings (Fig. 2; Pl. 1, 2, 3). The palynoassemblage recorded in the section represents a large range of angiosperms assigned to families including Arecaceae, Araceae, Annonaceae, Alangiaceae, Thymeleaceae, Bombacaceae, and Anacardiaceae, and pteridophytes of Cyathaceae, Schizaeaceae, Gleicheniaceae, Polypodiaceae, and Matoniaceae. Table 2 describes their habitats and distribution, assigned on the basis of the ecological niches of similar extant taxa (Tryon & Tryon 1982, Thankaimoni et al. 1984, Venkatachala et al. 1989, Kumar 1996, Collinson 2002).

The habitat and climatic preferences of the fossil taxa and their close relationship with modern plants indicate the existence of lowland tropical forest in the region. Pteridophyte spores of Schizaeaceae (*Lygodiumsporites* spp.), Gleicheniaceae (*Dictyophyllidites kyrtomatus*), and Polypodiaceae (*Polypodiaceaesporites repandus*) suggest the constant presence of water in the close vicinity of the deposition site. The occurrence of *Spinizonocolpites echinatus* (=*Nypa fruticans*, Arecaceae) and the fern *Acrostichumsporites meghalayaensis* (=*Acrostichum aureum*) in the middle and upper sequences indicate mangrove-type vegetation. The wide spectrum of recovered fossil pollen grains contains the palm taxa *Arengapollenites* (=*Arenga*), *Arecipites* spp. (=*Phoenix* sp.), and *Longapertites vaneedenburgi* (=*Eugissona*). The variety and abundance of palm genera represent a model group for tropical rain forest evolution (Sahni 2006, Couvreur et al. 2011) and indicate

Table 2. Ecological and geographical distribution of some extant taxa, and their affinity with fossil palynotaxa

Palynotaxa	Botanical affinity and family	Habitat	Distribution
Cyathidites australis	*Cyathea* (Cyatheaceae)	Along swamps and river streams	Tropical wet montane forests
Lygodiumsporites spp.	Schizaeaceae	Along river or stream banks	Tropical to subtropical regions
Dictyophyllidites kyrtomatus	Gleicheniaceae	Wet places, e.g. swamps and river banks	Tropical to subtropical regions
Acrostichumsporites meghalayaensis	*Acrostichum aureum* (Pteridaceae)	Along deltaic coast	Tropical to subtropical regions
Dandotiaspora telonata, *D. plicata*	Matoniaceae	As underground rhizome in marshy areas	Cosmopolitan
Polypodiaceaesporites repandus	Polypodiaceae	In cracks of rocks and at bases of trees	Tropical rainforests
Neocouperipollis kutchensis	Arecaceae	Along coastal areas	Tropical to subtropical forests
Palmaepollenites spp.	Arecaceae	Coastal swamps	Tropical to subtropical evergreen forests
Palmidites plicatus	Arecaceae	Lowlands, steeps of hillocks	Tropical to subtropical forests of India and SE Asia
Arengapollenites ovatus	*Arenga pinnata* (Arecaceae)	Grows wild in low elevated regions	Forests of north-east India and SE Asia
Arecipites bellus and *A. wodehousei*	Arecaceae	Coastal warm regions	Tropical rainforests
Longapertites vaneedenburgi	(Eugissona) Arecaceae	Low-lying shrubby forests and swamps	Tropics of South-east Asia
Proxapertites microreticulatus	Araceae	Moist regions	Tropical, subtropical to temperate
Spinizonocolpites echinatus	*Nypa fruticans* (Arecaceae)	Mangroves along deltaic coast	Tropical to subtropical regions
Matanomadhiasulcites maximus	Annonaceae	Semi-humid regions adjacent to coast	Tropical lowland evergreen forests
Lanagiopollis ruguloverrucatus	Alangiaceae	Moist lowland areas	Tropical woodland forest
Clavaperiporites heteroclavatus	Thymeleaceae	Along coastal margins	Tropical forests
Lakiapollis ovatus, *L. microreticulatus*	*Durio* (Bombacaceae)	Swamp and lowland areas	Tropical to subtropical evergreen forests
Rhoipites kutchensis	Anacardiaceae	Coastal habitats	Tropical to subtropical forests

dense and diversified vegetation characteristic of tropical climate. Recovered fossil pollen grains of *Matanomadhasulcites maximus* (Annonaceae), *Clavaperiporires heteroclavatus* (Thymeleaceae), and *Lakiapollis ovatus* (Bombacaceae) in the assemblage represent megathermal families (Morley 2000) distributed mostly in equatorial regions. Fruiting bodies of Microthyriaceae fungi, commonly occurring in tropical and subtropical areas of the world, are associated with vegetation that thrives in the warm humid climate of tropical and subtropical regions (Dilcher 1965). The presence of fungal fruiting bodies of the family Microthyriaceae (e.g. *Callimothallus*, *Phragmothyrites*) indicates that warm humid climate with heavy precipitation prevailed during deposition of the lignite.

SEDIMENTARY ORGANIC MATTER (PALYNOFACIES)

The term ‘palynofacies’ refers to all acid-resistant plant organic matter, recovered from sediments by palynological processing techniques using dilute HCl and HF (Combaz 1964). The composition of sedimentary organic matter reflects the variety of environmental conditions and also suggests a certain level of potential for hydrocarbon generation (Powell et al. 1990, Batten 1996). The degree of preservation or biodegradation of organic matter depends on its quantity, the availability of minerals, and the physical conditions that prevailed during its deposition in the basin (Demaison & Moore 1980, Philp 1981). Table 3 lists the sedimentary organic matter (palynofacies), classified according to Masran and Pocock (1981), Pocock et al. (1988), and Batten (1996).

DISTRIBUTION OF SEDIMENTARY ORGANIC MATTER (SOM) IN STRATA

The relative abundance of various types of sedimentary organic matter (structured terrestrial, biodegraded terrestrial, amorphous, resins, black debris, palynoflora, microforaminiferal linings) is given in Figure 3, and the types are pictured in Plate 4. Phytoclasts are preserved in various lithotypes forming organic-rich sediments, and they are characteristic of oxic-dysoxic and anoxic facies. The palynofacies of various sedimentary sequences are dominated mainly by terrestrial components transported from nearby forested areas. The organic matter types are distributed among the various sedimentary intervals as follows:

Samples 1–14 (0–5.2 m)

Description. Thick basal lignite seam (0–5.2 m) with a carbonaceous shale parting (~0.5 m), showing dominance of resin globules (15–45%), followed by biodegraded terrestrial (20–25%) and amorphous (5–25%) organic matter, and black debris which declines from 35% to 25% from the base to the middle part of lignite.

Interpretation. The uniform distribution of biodegraded terrestrial, amorphous organic matter, and black debris indicates dysoxic conditions during their burial. Abundant angiosperm pollen grains of families such as Arecaceae, Annonacaeae, and Bombacaceae (*Durio* type), with abundant fungal fruiting bodies, are recorded in this interval.

Samples 15–23 (5.3–7.5 m)

Description. Carbonaceous shale with lignite parting, showing dominance of black debris (65%), gradually declining to 50% in the upper part, followed by biodegraded terrestrial (20–10%) and amorphous matter (2–5%); resin increases in frequency from 30% to 40% in this interval.

Interpretation. The abundance of black debris versus biodegraded and amorphous organic matter indicates oxic conditions of burial at the sediment/water interface. The recovered material includes pollen grains of various families such as Arecaceae and Bombacaceae,

Table 3. Palynofacies types, characteristics and inferred depositional environments of material from the Surkha lignite mine section

Palynofacies type	Characteristics	Environment
Structured terrestrial organic matter	Discrete particles (of e.g. leaf, wood, root) showing well preserved cell patterns	Low-energy fluvial-deltaic and lacustrine environments
Biodegraded terrestrial organic matter	Pale to brown weakly structured biodegraded phytoclasts with indefinite outline, produced as a result of partial to moderate activity of microbes (fungi, bacteria) on various plant organs	Burial under dysoxic to oxic environments
Amorphous organic matter	Completely structureless organic matter, pale yellow to light brown, appearing as fluffy mass due to microbial activity (fungi, bacteria)	Anoxic environment (Venkatachala 1981, Tyson 1989, 1995, Pacton et al. 2011)
Resins	Cell secretions of higher plants with globular structures varying in shape from semi-spherical to spherical, irregular or rod-shaped, smooth, pitted or with concoidal fractures	Fluvial, deltaic or near-shore deposits
Black debris	Dark brown to black, opaque with sharply distinct or indefinitely outlined phytoclasts, produced by oxidation of plant tissues	Oxic environmental conditions (Oboh-Ikuanobe & Villiers 2003)
Fungi	Fungal hyphae, ascomata, sclerotia, spores, and other reproductive parts, indicating infestation on land-derived phytoclasts	Variable depositional environments under warm and humid conditions
Spores and pollen grains	Palynomorphs of pteridophytes and angiosperms	Terrestrial depositional environment
Freshwater and marine microalgae	Spores of *Spirogyra* (*Psiloschizosporis* sp.), other filamentous freshwater algae, and dinoflagellate cysts, indicating influx of sediments from terrestrial or marine sources	Freshwater algae (Chlorophyceae) and dinoflagellate cysts indicate proximity to shore with marine transgressive and regressive phases (Habib & Miller 1989, Habib et al. 1994)
Microforaminiferal linings	Organic remains of small (<150 µm) foraminifers, oval or crescent-shaped chambers arranged in helical patterns	Potential indicator of marine sources (Wilson & Hoffmeister 1952, Stancliffe 1989)

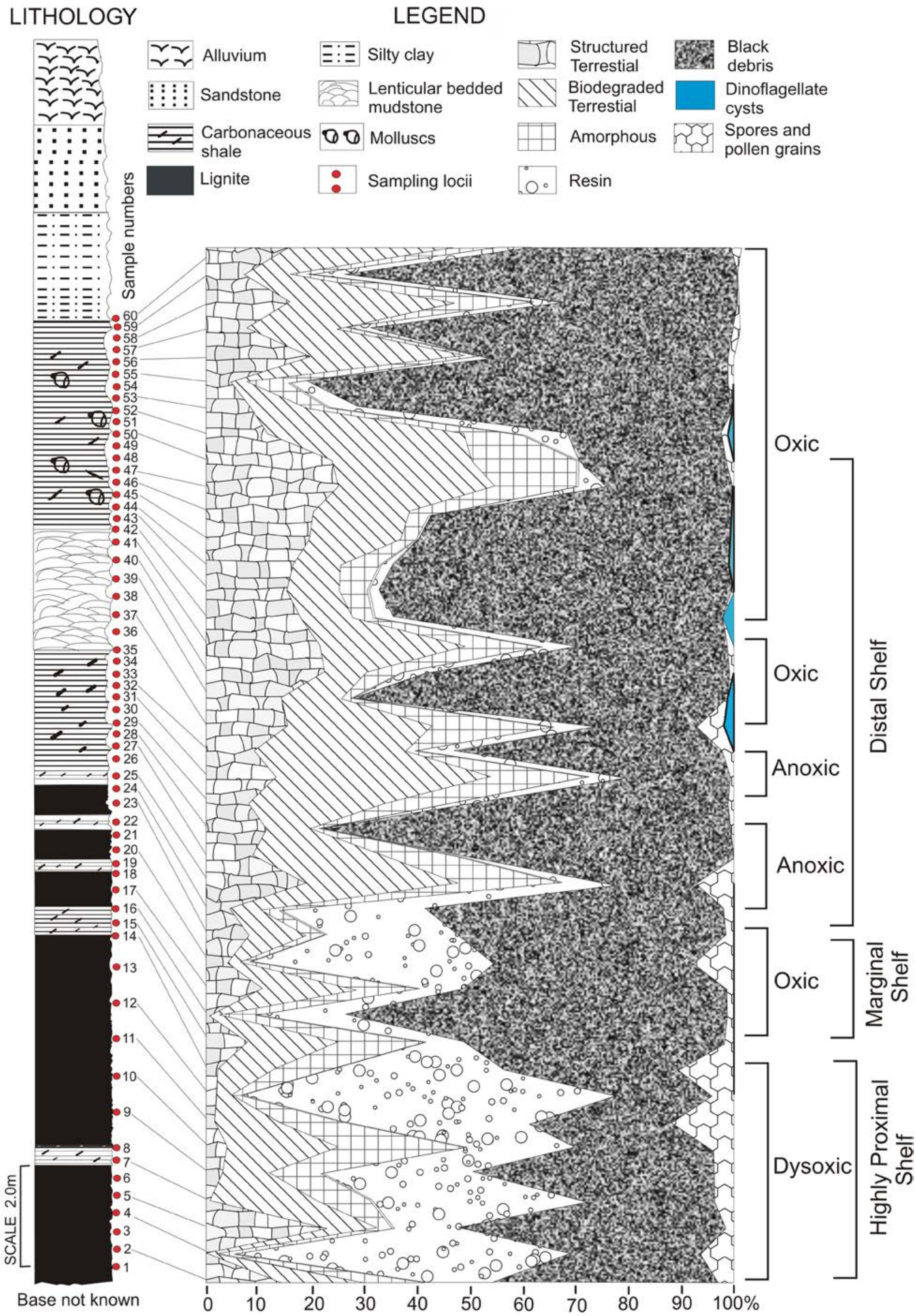

Fig. 3. Quantitative representation of sedimentary organic matter (palynofacies) and their burial conditions

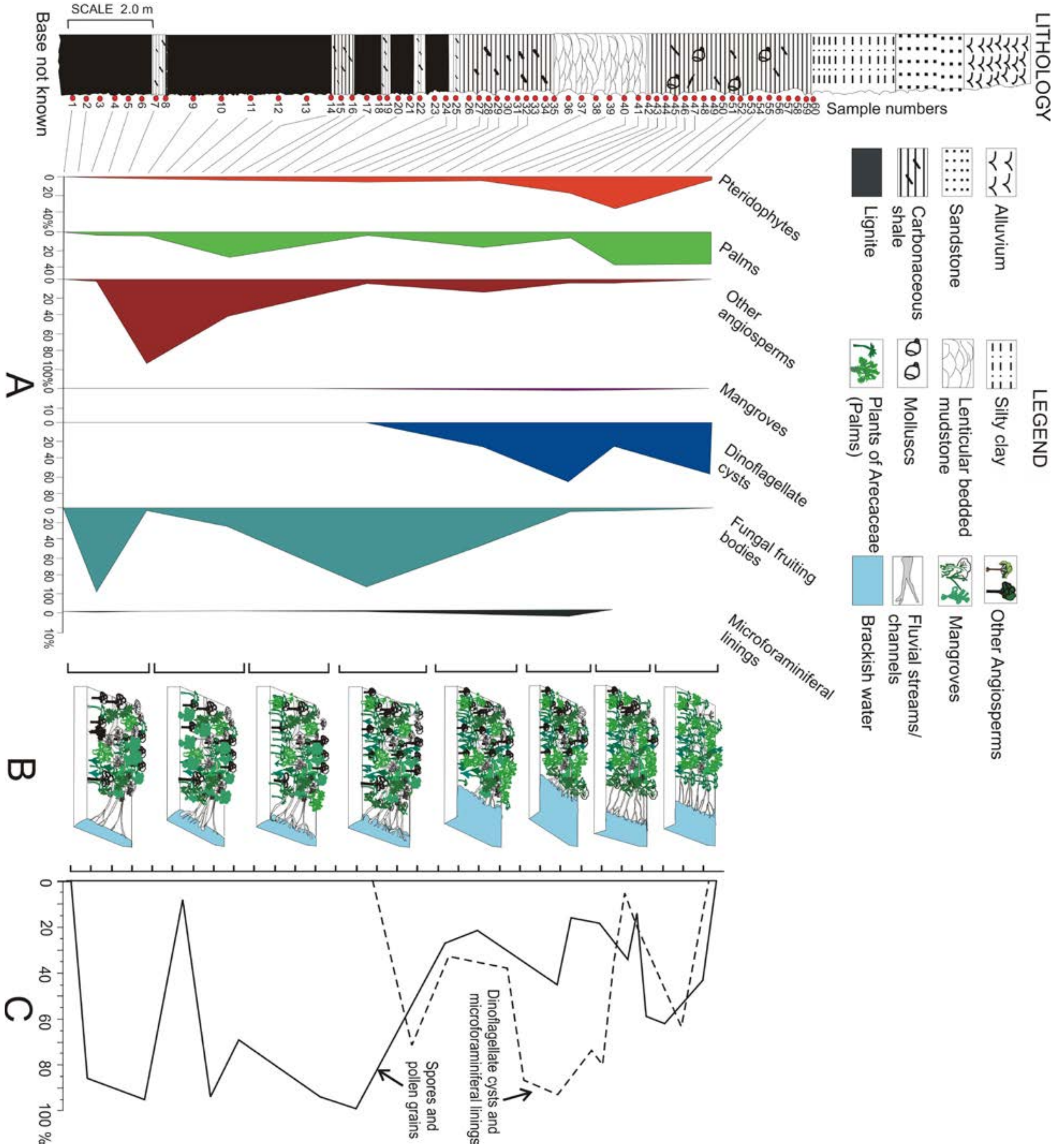

Fig. 4. **A** – Distribution of various groups of taxa, **B** – succession of vegetation, and **C** – comparative frequency of terrestrial and marine palynomorphs

pteridophyte spores of Matoniaceae and Polypodiaceae, the mangrove fern *Acrostichumsporites meghalayaensis* of Pteridaceae, and significant dinoflagellate cysts of *Homotryblium tenuispinosum*, *H. abbreviatum*, and *Cordosphaeridium fibrospinosum*, along with fungal remains.

Samples 24–32 (7.6–9.8 m)

Description. This interval consists of finely laminated carbonaceous shale 2.2 m thick. The lower part (7.6–8.3 m, samples 24–28) shows dominance of biodegraded terrestrial (35%) followed by amorphous (20%) organic matter, black debris declining from 50% at the base to 20% in the middle, and resins (8%). The upper part (8.4–9.2 m, samples 29–32) shows 40% biodegraded terrestrial and 20% amorphous organic matter, and 75% black debris decreasing to 40% towards the top.

Interpretation. The carbonaceous shale indicates anoxic conditions of deposition and associated microbial activity, with abundant biodegraded and amorphous organic matter. In the lower part of this carbonaceous shale, dinoflagellate cysts of *Homotryblium tenuispinosum*, *H. abbreviatum*, and *Cordosphaerdium fibrospinosum* continue in abundance, with fewer pollen grains of Arecaceae and Annonaceeae, while the upper part shows the peak of dinoflagellate cysts of *Homotryblium* spp., followed by *Cordosphaeridium fibrospinosum*, *C. exilimurum*, and others.

Samples 36–41 (9.9–11.6 m)

Description. The interval consists of lenticular bedded mudstone rich in black debris (70%), with structured terrestrial (20–25%), biodegraded (15–30%) and amorphous (10%) organic matter.

Interpretation. The interval shows oxic burial conditions owing to the large presence of black debris and structured terrestrial organic matter. Dinoflagellate cysts continue to appear, with fewer pollen grains of Arecaceae and abundant spores of Gleicheniaceae.

Samples 42–60 (11.7–14.8 m)

Description. Overlying carbonaceous shale with biodegraded terrestrial organic matter declining from 35% to 25%, amorphous organic matter declining from 10% to 5% towards the top, and black debris increasing from 80% to 85% in this facies.

Interpretation. This phase again shows oxic burial conditions, with black debris much more abundant than biodegraded terrestrial and amorphous organic matter. The frequency of dinoflagellate cysts significantly declines, while spores of Cyatheaceae, Matoniaceae, and Gleicheniaeceae appear in significant amounts.

UV FLUORESCENCE OF SEDIMENTARY ORGANIC MATTER (SOM)

SOM from the various lithotypes showed weak to moderate responses under UV light, seen in the images of Plate 4. A majority of leaf cuticles showed more intense yellow fluorescence, while partially biodegraded terrestrial organic matter fluoresced pale yellow. The resins and amorphous organic matter showed moderate to intense fluorescence due to the heterogeneity of their constituents (Pacton et al. 2011). The variable response of sedimentary organic matter under UV fluorescent light in sediments of the Cambay shale around the Surkha mining area indicates moderate to weak hydrocarbon generation potential.

The burial of sedimentary organic matter in various depositional settings – proximal, marginal, and distal shelves (Fig. 3) – is explained as follows:

a) Proximal shelf: The proximal shelf occurs in samples 1–14. The shelf contains sedimentary organic matter derived from terrestrial sources, with abundant pollen grains. The SOM contains the highest percentage of black debris (40–50%) at the bottom and 40% in the upper part, followed by resin globules (10–60%), amorphous (10–15%), biodegraded terrestrial (18–20%), and structured terrestrial (3–4%) organic matter, indicating dysoxic-oxic burial conditions.

b) Marginal shelf: The carbonaceous shale alternating with lignite in the middle part of the section (samples 15–20) contains spores and pollen grains. The SOM is rich in black debris (73% to 55%) towards the top, followed by biodegraded terrestrial (10–15%) and amorphous (8–3%) organic matter, resin (12–27%), and structured terrestrial (8–10%) organic matter, indicating oxic burial conditions.

c) Distal shelf: The 8.0 m thick section (samples 21–50) comprises carbonaceous shale with lignite parting (1.3 m), carbonaceous shale (2.6 m), and lenticular bedded mudstone (2.0 m) in the upper part, and overlying carbonaceous shale in the lower part (2.0 m). The shelf is rich in dinoflagellate cysts, followed by pteridophyte spores and pollen grains. The fluctuation of SOM abundance between samples indicates alternating anoxic facies (samples 21–32) and oxic facies (samples 33–50).

DEPOSITIONAL ENVIRONMENT

Our palynostratigraphic and palynofacies analyses indicate the depositional environments of the lignite-bearing sequences at Surkha in the Cambay Basin. The floristic changes observed in the section exhibit a changing pattern of material supply from freshwater streams and marine sources. Initially, an enormous quantity of plant biomass from nearby vegetation around the swamp was transported by streams and accumulated in the deposition area, resulting in peat formation under low energy and reducing conditions. These conditions generally prevailed in slowly subsiding basin margins far from the river mouth and in other places along the coast where sediments were deposited very rapidly (Lütting 1977). The thick lignite beds at the base suggest that the accommodation space created due to a rise in the level of the base was in equilibrium with the growth of the marsh that supplied the organic matter. Most lignite deposits are presumed to have been formed in lowland coastal swamp between marine and continental facies belts (Steininger et al. 1989).

We also assessed the temporal variation of the vegetation pattern between stratigraphic levels in terms of the changing depositional environmental conditions. In the basal part of the succession the main palynological constituents are bushy plants of Annonaceae (*Matanomadhiasulcites maximus*) and Bombaceae (*Durio=Lakiapollis ovatus*). Later the palynoassemblage suggests that the region was occupied by abundant arboreal plants of Bombacaceae (*Lakiapollis ovatus*, *L. matanomadhiensis*), Alangiaceae (*Lanagiopollis ruguloverrcatus*), and mid-story palms (e.g. *Arengapollenites achinatus*, *Longapertites vaneedenburgi*, *Arecipites bellus*, *Palmidites plicatus*, *Palmaepollenites kutchensis*, *P. nadhamunii*), with other pollen grains of *Clavaperiporites heteroclavatus* (=*Wikstroemia indica* of the family Thymeleaceae) and freshwater alga (*Psiloschizosporis* sp.). The profuse fossil pollen of *Lakiapollis ovatus* morphologically resembles the pollen of *Durio* (Bombacaceae) now growing in the Indo-Malayan Tropics (Thanikaimoni et al. 1984). The present-day distribution pattern mostly covers tropical megathermal forest zones. The presence of mangrove taxa *Acrostichumsporites meghalayaensis* (=*Acrostichum aureum*) and *Spinizonocolpites echinatus* (=*Nypa fruticans*) in the *Arecipites wodehousei* cenozone, and shallow marine forms (dinoflagellate cysts and microforaminiferal linings) in the *Homotryblium tenuispinosum* cenozone, suggests a strong marine influence resulting from a marine transgression. The topmost *Homotryblium tenuispinosum* palynozone indicates a substantial rise of sea level which must have flooded the coastal marshes and completely halted peat formation.

A comparison of the abundance of terrestrial and marine palynomorphs documented in the stratigraphic column helps to reveal the palaeoenvironmental changes in the area (Fig. 4C). The plants occupied varied ecological niches. The palynozones represent the vegetation successions and sediment accumulation under three phases of deposition. The first phase, dominated by the *Matanomadiasulcites maximus* cenozone and *Lakiapollis ovatus* cenozone in a low-lying coastal zone, indicates deposition of sediments in a freshwater swamp environment. The second phase, marked by the *Arecipites wodehousei* cenozone, was a transition phase, suggesting a brackish lagoonal environment of deposition. In the third phase, in the upper part of the sedimentary succession, the coastal swamp was flooded by marine water as a result of a marine transgression; an estuarine environment developed, seen in the large number of preserved dinoflagellate cysts. The increase in the abundance of pteridophyte spores in the upper part of the succession indicates that pteridophytes were growing vigorously due to increased moisture in and around the depositional environment.

CONCLUSIONS

1. The palynoflora and sedimentary organic matter recorded in the succession of the Surkha lignite mine, Cambay Basin, provide important insights into stratigraphic changes in the palynoflora, vegetation, and climate of the tropical zone during the early Eocene (Ypresian).

2. The palynological data suggest a warm and humid tropical-subtropical climate which favoured the growth of coastal palms and evergreen arboreal angiosperms close to the site of deposition.

3. The data obtained show temporal fluctuation of pollen and dinoflagellate cyst content. Three phases of deposition are recognised. In Phase I, the lower part of the lignite succession, deposition took place in a lowland coastal swamp environment. In Phase II, middle carbonaceous shales, deposition took place in a lagoonal environment. In Phase III, the carbonate-rich muddy shales of the upper part of the sequence, deposition took place in an estuarine environment. Generally, deposition took place in proximal to distal shelf conditions.

4. The palynofacies data indicate high terrestrial input in the lignite-bearing sequences, and their burial in various oxic-dysoxic and anoxic facies. The fluorescence images of the phytoclasts indicate that the sediments are of moderate to weak hydrocarbon generation potential.

5. Overall, the composition of the palynoflora demonstrates the regional presence of large numbers of tropical megathermal plant families, and shows much similarity with the lowland tropical environment of the Indian subcontinent.

ACKNOWLEDGEMENTS

We are grateful to Prof. Sunil Bajpai (Director, Birbal Sahni Institute of Palaeobotany, Lucknow) for providing facilities for this work and for granting a permit (BSIP/RDCC no. 78/2014-2015). We thank P.K. Samantray (Senior Manager, Surkha Lignite Mine Project) for his assistance, and the Directorate of Geology and Mining (Gujarat) for providing the necessary facilities for collection of sediment samples.

REFERENCES

AGRAWAL C.G. 1986. Structure and tectonics of exposed rocks between Narmada and Kim rivers in South Gujarat. J. Geol. Soc. India, 27: 531–542.

BAJPAI S., KAPUR V.V., DAS D.P., TIWARI B.N., SARVANAN N. & SHARMA R. 2005a. Early Eocene land mammals from Vastan Lignite Mine, District Surat (Gujarat), western India. J. Palaeontol. Soc. India, 50(1): 101–113.

BAJPAI S., KAPUR V.V., THEWISSEN J.G.M., TIWARI B.N., DAS D.P., SHARMA R. & SARVANAN N. 2005b. Early Eocene primates from Vastan Lignite Mine, Gujarat, western India. J. Palaeontol. Soc. India, 50(2): 43–54.

BANERJEE A., JHA M., MITTAL A., THOMAS N.J. & MISRA K.N. 2000. The effective source rocks in the north Cambay Basin, India. Marine and Petrol. Geol., 17: 1111–1129.

BATTEN D.J. 1996. Palynofacies and palaeoenvironmental interpretation: 1011–1064. In: Jansonius J., McGregor D.C. (eds), Palynology, Principals and Applications. Am. Ass. Strat. Palynol. Foundation, Dallas.

BATTEN D.J. & MORRISON L. 1983. Methods of palynological preparation for palaeoenvironmental, source rock and organic maturation studies. Norweg. Petrol. Direct. Bull., 2: 35–53.

BESEMS R.E. 1993. Dinoflagellate cyst biostratigraphy of Tertiary and Quaternary deposits of offshore NW Borneo. Geol. Soc. Malaysia Bull. 33: 65–93.

BHANDARI L.L. & CHOUDHARY L.R. 1975. Stratigraphical Analysis of Kadi and Kalol Formation, Cambay Basin, India. Am. Assoc. Petrol. Geol. Bull., 59: 856–871.

BHANDARI A. & RAJU D.S.N. 2000. Palaeogene biofacies, palaeoecology and sea level fluctuations in Tarapur-Cambay Block, India. Bull. Oil Nat. Gas Corp., 37: 197–213.

BROWN C.A. 1960. Palynological techniques. Baton Rouge, LA.

BUJAK J.P., DOWNIE C., EATON G.L. & WILLIAMS G.L. 1980. Dinoflagellate Cysts and Acritarchs from the Eocene of Southern England. Spl. Papers Palaeontol., 24: 1–100.

COLLINSON M.E. 2002. The ecology of Cainozoic ferns. Rev. Palaeobot. Palynol., 119: 51–68.

COMBAZ A. 1964. Les Palynofacies. Rev. Micropaleontol., 7: 205–218.

COUVREUR T.L.P., FOREST F. & BAKER W.J. 2011. Origin and global diversification patterns of tropical rainforests: inferences from a complete genus-level phylogeny of palms. BMC Bio., 9: 1–12.

CROUCH E.M., DICKENS G.R., BRINKHUIS H., AUBRY M.-P., HOLLIS C.J., ROGERS K.M., VISSCHER H. 2003. The Apectodinium acme and terrestrial discharge during the Paleocene–Eocene thermal maximum: new Palynological, geochemical and calcareous nannoplankton observations at Tawanui, New Zealand. Palaeogeogr., Palaeoclimatol., Palaeoecol., 194: 387–403.

DAYAL A.M., MANI D., MISRA S. & PATIL D.J. 2013. Shale gas prospective of the Cambay Basin, Western India. Geohorizons, January, 2013: 26–31.

DEMAISON G.J. & MOORE G.T. 1980. Anoxic Environments and oil source bed genesis. Am. Assoc. Petrol. Geol. Bull., 64(8): 1179–1209.

DILCHER D.L. 1965. Epiphyllous Fungi from Eocene Deposits in Western Tennessee, U.S.A. Palaeontographica, B, 116: 1–54.

EDWARDS L.E. 2007. Palaeocene and Eocene Dinocysts from the Salt Range, Punjab, Northern Pakistan. In: Warnick P.D & Wardlaw B.R. (eds), Regional studies of the Potwar Plateau Area, Northern Pakistan. U.S. Geol. Surv. Bull., 2078: C1–C10.

GARG R., PRASAD V., THAKUR B., SINGH I.B. & ATEEQUZZAMAN K. 2011. Dinoflagellate cysts from the Naredi Formation, South western Kutch, India: implication on age and palaeoenvironment. J. Palaeontol. Soc. India, 56(2): 201–218.

GARG R., ATEEQUZZAMAN K., PRASAD V., TRIPATHI S.K.M., SINGH I.B., JAUHRI A.K. & BAJPAI S. 2008. Age-diagnostic dinoflagellate cysts from the lignite-bearing sediments of the Vastan lignite mine, Surat District, Gujarat, Western India. J. Palaeontol. Soc. India, 53: 99–105.

HABIB D. & MILLER J.A. 1989. Dinoflagellate species and organic facies evidence of marine transgression and regression in the Atlantic Coastal Plain. Palaeogeogr. Palaeoclimatol. Palaeoecol., 74: 23–47.

HABIB D., ESHET Y. & VAN PELT R. 1994. Palynology of sedimentary cycles: 311–335. In: Traverse A. (ed.), Sedimentation of Organic particles. Cambridge University Press, Cambridge.

IAKOVLEVA A.I., BRINKHUIS H. & CAVAGNETTO O.C. 2001. Late Palaeocene–Early Eocene dinoflagellate cysts from the Turgay Strait, Kazakhstan; correlations across ancient seaways. Palaeogeogr., Palaeoclimatol., Palaeoecol. 172(3,4): 243–268.

KAR R.K. 1985. The fossil floras of Kachchh IV. Tertiary palynostratigraphy. The Palaeobotanist, 34: 12–80.

KAR R.K. & BHATTACHARYA M. 1992. Palynology of Rajpardi Lignite, Cambay Basin, Gujra Dam and Akri Lignite, Kutch Basin. The Palaeobotanist, 39(2): 250–263.

KING C., IAKOVLEVA A.I., STEURBAUT E., HEILMANN-CLAUSEN C. & WARD D. 2013. The Aktulagay section, west Kazakhstan: a key site for northern mid-latitude Early Eocene stratigraphy. Stratigraphy, 10(3): 171–209.

KUMAR M. 1996. Palynostratigraphy and palaeoecology of Early Eocene palynoflora of Rajpardi lignite, Bharuch District, Gujarat. The Palaeobotanist, 43(3): 110–121.

LARSSON L.M., VAJDA V. & RASMUSSEN E.S. 2006. Early Miocene pollen and spores from western Jylland, Denmark-environmental and climatic implications. GFF, 128: 261–272.

LÜTING G. 1977. A general view of the Neogene and Quaternary of the Mediterranean with respect to lignite prospecting: 1199–1216. Proc.VI. Coll. Geol. Aegean Region, Inst. Geol. Min. Res., Athens.

MADHAVI T., KUMAR T.S., RASHEED M.A., KALPANA.G., PATIL D.J. & DAYAL A.M. 2009. Light hydrocarbons geochemistry of surface sediment from petroliferous region of the Mehsana Block, North Cambay Basin. J. Geol. Soc. India, 74: 7–15.

MANDAL J. & GULERIA J.S. 2006. Palynology of Vastan lignite (Surat District), Gujarat: its age, palaeoecology and depositional environment. The Palaeobotanist, 55: 51–66.

MASRAN T.C. & POCOCK S.A.J. 1981. The classification of plant derived particulate organic matter in sedimentary rocks: 145–175. In: Brooks J. (ed.), Organic maturation studies and fossil fuel exploration. Academic Press, London.

MOHAN M. 1995. Cambay Basin – A promise of oil and gas potential. J. Palaeontol. Soc. India, 40: 41–47.

MORLEY R.J. 2000. Origin and Evolution of Tropical Rain Forest. John Wiley and Sons Ltd, Chichester.

NAGORI M.L., KHOSLA S.C. & JAKHAR S.R. 2013. Middle Eocene Ostrocoda from the Tadkeshwar Lignite Mine, Cambay Basin, Gujarat. J. Geol. Soc. India, 81: 514–520.

OBOH-IKUENOBE F.E. & VILLIERS S.E. 2003. Dispersed organic matter in samples from the western continental shelf of Southern Africa: palynofacies assemblages and depositional environments of Late Cretaceous and younger sediments. Palaeogeogr., Palaeoclimatol. Palaeoecol., 201: 67–88.

PACTON M., GORIN G.E. & VASCONCELOS C. 2011. Amorphous organic-matter experimental data on formation and the role of microbes. Rev. Palaeobot. Palynol., 166: 253–267.

PHILP R.P. 1981. Diagenetic organic matter in recent sediments and environments of deposition. BMR J. Australian Geol. Geophys., 6: 301–306.

POCOCK S.A.J., VASANTHY G. & VENKATACHALA B.S. 1988. Introduction to the study of particulate organic materials and ecological perspectives. J. Palynol., 23–24: 167–188.

POTONIÉ R. & KREMP G.O.W. 1955. Die Sporae dispersae des Ruhrkarbons ihre Morphographie und Stratigraphie mit Ausblicken auf Arten anderer Gebiete und Zeitabschnitte. Teil I. Palaeontographica, B, 98: 1–136.

POTONIÉ R. & KREMP G.O.W. 1956. Die Sporae dispersae des Ruhrkarbons ihre Morphographie und Stratigraphie mit Ausblicken auf Arten anderer Ggebiete und Zeitabschnitte. Teil. II. Palaeontographica, B, 99: 85–191.

POWELL A.J. 1992. Dinoflagellate cysts of the Tertiary System: 155–251. In: Powell A.J. (ed.), A Stratigraphic index of Dinoflagellate Cysts. British Micropalaeontol. Soci. Publ. Ser., Kluwer Academic Publishers, Dordrecht, The Netherlands.

POWELL A.J., DODGE J.D & LEWIS J. 1990. Late Neogene to Pleistocene palynological facies of the Peruvian Continental Margin upwelling, Leg 112: 297–321. In: Suess E., von Huene R. et al. (eds), Proc. of the Ocean Drilling Program, Scientific Results.

PRASAD V., FAROOQUI A., TRIPATHI S.K.M., GARG R., THAKUR B. 2009. Evidence of Late Palaeocene–Early Eocene equatorial rain forest refugia in southern Western Ghats India. J Biosci., 34: 777–797.

PRASAD V., SINGH I.B., BAJPAI S., GARG R., THAKUR V., SINGH A., SARAVANAM N. & KAPUR V.V. 2013. Palynofacies and sedimentology-based high-resolution sequence stratigraphy of the lignite-bearing muddy costal deposits (early Eocene) in the Vastan Lignite Mine, Gulf of Cambay, India. Facies, 59: 737–761.

RANA R.S., KUMAR K. & SINGH, H. 2004. Vertebrate fauna from the subsurface Cambay Shale (Lower Eocene), Vastan Lignite, Gujarat India. Curr. Sci., 87: 1726–1733.

RAO M.R., SAHNI A., RANA R.S. & VERMA P. 2013. Palynostratigraphy and depositional environment of Vastan lignite mine (Early Eocene), Gujarat, western India. J. Earth Syst. Sci., 122(2): 289–307.

SAHNI A. 2006. Biotic response to the India-Asia collision: Changing palaeoenvironment and vertebrate faunal relationship. Palaeontographica, A, 278: 15–26.

SAMANT B. & MOHABEY D.M. 2005. Response of flora to Deccan volcanism: A case study from Nand–Dongargaon basin of Maharastra, Implications to environment and climate. Gond. Geol. Magz., Spl. Vol. 8: 151–164.

SAMANT B. & MOHABEY D.M. 2014. Deccan volcanic eruptions and their impact on flora: Palynological evidence: 171–191. In: Keller G. & Kerr A.C. (eds), Volcanism, Impacts, and Mass Extinctions: Causes and Effects. Geo. Soc. America Spl. Paper, 505.

SAMANT B. & PHADTARE N.R. 1997. Stratigraphic palynoflora of the Early Eocene Rajpardi lignite, Gujarat and the lower age limit of the Tarkeshwar Formation of South Cambay Basin, India. Palaeontographica, B, 245: 1–108.

SIVAN P., DATTA G.C., & SINGH R.R. 2008. Aromatic biomarkers as indicators of source, depositional environment, maturity and secondary migration in the oils of Cambay Basin, India. Organic Geochem., 39: 1620–1630.

STANCLIFFE R.P.W. 1989. Microforaminiferal linings: their classification, biostratigraphy and palaeoecology with special reference to specimens from British Oxfordian sediments. Micropalaeontol., 35: 337–352.

STAPLIN F.L. 1969. Sedimentary organic matter, organic metamorphism, and oil and gas occurrences. Bull. Can. Petrol. Geol., 17: 47–66.

STEININGER F.F., RÖEGL F., HOCHULI P. & MÜLLER C. 1989. Lignite deposition and marine cycles. The Austrian Tertiary lignite deposits: a case history. Sitzber. Österr. Akad. Wiss., Math.-Naturwiss. Kl. Abt. I, 197: 309–332.

THANIKAIMONI G., CARATINI C., VENKATACHALA B.S., RAMANUJAM C.G.K. & KAR R.K. 1984. Selected Tertiary angiosperm pollen from India and their relationship with African Tertiary pollen. Inst. Fr. Pondicherry Trav. Sec. Scient. Techn., 19: 1–93.

TORRICELLI S., KNEZAUREK G. & BIFFI U. 2006. Sequence biostratigraphy and palaeoenvironmental reconstructions in the Early Eocene Figols Group of the Tremp-Graus Basin (south-central Pyrenees, Spain). Palaeogeogr. Palaeoclimatol. Palaeoecol., 232: 1–35.

TRAVERSE A. 1988. Palaeopalynology. Unwin Hyman, Boston.

TRIPATHI S.K.M. & SRIVASTAVA D. 2012. Palynology and palynofacies of the early Palaeogene lignite bearing succession of Vastan, Cambay Basin, western India. Acta Palaeobot., 52(1): 157–175.

TRYON R.M. & TRYON A.F. 1982. Ferns and Allied Plants with special reference to Tropical America. Springer-Verlag, New York, Heidelberg, Berlin.

TYSON R.V. 1989. Late Jurassic palynofacies trends, Piper and Kimmeridge Clay Formations, UK onshore and offshore northern North Sea: 135–172. In: Batten D.J. & Keen M.C. (eds), Northwest European Micropalaeontology and Palynology, Ellis Horwood, Chichester.

TYSON R.V. 1995. Sedimentary Organic Matter, Organic Facies and Palynofacies. Chapman and Hall, London.

VAN GIJZEL P. 1982. Characterization and identification of kerogen and bitumen and determination of thermal maturation by means of qualitative and quantitative microscopial techniques: 1–46. In: Staplin F.L., Dow W.G., Milner C.W.D., O'Connor D.I., Pocock S.A.J., van Gijzel P., Welte D.H. & Yükler M.A. (eds), How to assess maturation and palaeotemperatures. SEPM Short Course Notes, 7.

VENKATACHALA, B.S. 1981. Differentiation of amorphous organic types in sediments: 177–200. In: Brooks J. (ed.), Organic maturation studies and fossil fuel exploration. Academic Press, London.

VENKATACHALA B.S. & KAR R.K. 1969. Palynology of the Tertiary sediments of Kutch. 1. Spores and pollen from borehole no. 14. The Palaeobotanist, 17: 157–178.

VENKATACHALA B.S., CARATINI C., TISSOT C. & KAR R.K. 1989. Palaeocene-Eocene marker pollen from India and tropical Africa. The Palaeobotanist, 37(1): 1–25.

WILSON G.J. 1988. Palaeocene and Eocene dinoflagellate cysts from Waipawa, Hawkes Bay, New Zealand. New Zealand Geol. Surv. Palentol. Bull. 57: 1–12.

WILSON L.R. & HOFFMEISTER W.S. 1952. Small foraminifera. The Micropalaeontol. 6: 26–28.

WILLIAMS G.L., STOVER L.E. & KIDSON E.J. 1993. Morphological and stratigraphic ranges of selected Mesozoic-Cenozoic dinoflagellate taxa in northern hemisphere. Geol. Surv. Canada 92–10: 1–137.

WILLIAMS G.L., BRINKHUIS H., PEARCE M.A., FENSOME R.A., WEEGINK J.W. 2004. Southern Ocean and global dinoflagellate cyst events compared: index events for the Late Cretaceous–Neogene. Proceedings of the Ocean Drilling Project, Scientific Results, 189: 1–98.

WING S.L., HARRINGTON G.J., SMITH F.A., BLOCH J.I., BOYER D.M. & FREEMAN K.H. 2005. Transient floral change and rapid global warming at the Paleocene-Eocene boundary. Science, 310: 993–996.

ZACHOS J., PAGANI M., SLOAN L., THOMAS E. & BILLUPS K. 2001. Trends, rhythms and aberrations in global climates 65 Ma to present. Science, 292: 686–693.

PLATES

Plate 1

1. *Polypodiaceaesporites levis* (Sah) Venkatchala & Rawat, BSIP slide no. 15280, T23/1
2. *Polypodiaceaesporites repandus* Takahashi, BSIP slide no. 15280
3. *Dandotiaspora plicata* Sah, Kar & Singh, BSIP slide no. 15278, W35
4. *Dandotiaspora telonata* Sah, Kar & Singh, BSIP slide no. 15289, E34
5. *Acrostichumsporites meghalayaensis* Kar, BSIP slide no. 15303, L45/2
6. *Lygodiumsporites pachyexinus* Saxena, BSIP slide no. 15286, M48
7. *Palmaepollenites kutchensis* Venkatachala & Kar, BSIP slide no. 15310, R42/2
8. *Longapertites vaneedenburgi* Germeraad et al., BSIP slide no. 15280, R38
9. *Palmidites plicatus* Singh, BSIP slide no. 15280, R38/1
10. *Arecipites bellus* Sah & Kar, BSIP slide no. 15281, L44
11. *Proxapertites assamicus* (Sah & Dutta) Singh, BSIP slide no. 15289, S32
12. *Neocouperpollis kutchensis* (Venkatachala & Kar) Kumar, BSIP slide no. 15294
13. *Rhoipites kutchensis* Venkatachala & Kar, BSIP slide no. 15282, J44/4
14. *Spinizonocolpites echinatus* Muller, BSIP slide no. 15295, W47
15. *Tricolpites reticulatus* Cookson, BSIP slide no. 15276, E24
16. *Margocolporites tsukadii* Ramanujam, BSIP slide no. 15284
17. *Minutitricolpites minutus* (Sah & Kar) Kar, BSIP slide no. 15281
18. *Lakiapollis ovatus* Venkatchala, BSIP slide no. 15277, N29/3
19. *Retitribrevicolporites matanomadhensis* (Venkatchala & Kar) Kar, BSIP slide no. 15279, O86/2
20. *Lakiapollis matanomadhensis* Venkatachala & Kar, BSIP slide no. 15277, J29
21. *Tricolporopollis rubra* Dutta & Sah, BSIP slide no. 15282, R44/4
22. *Dermatobrevicolporites dermatus* Kar, BSIP slide no. 15281, L48/2
23. *Albertipollenites crassireticulatus* (Dutta & Sah) Mandal & Rao, BSIP slide no. 15286, F45/1
24. *Retipilonapites cenozoicus* (Sah) Saxena, BSIP slide no. 15285, J47
25. *Monosulcites sp.* (=*Ammandra decasperma*), BSIP slide no. 15287, T39/1
26. *Clavaperiporites ramanujamii* Samant & Phadtare, BSIP slide no. 15285, N22/3
27. *Retibaculipolycolpites baculatus* Kar & Sharma, BSIP slide no. 15284, O45/1
28. *Matanomadhiasulcites maximus* Kar, BSIP slide no. 15277, K37
29. *Lanagiopollis rugularis*, Morley, BSIP slide no. 15278, R34
30. *Lanagiopollis* sp. A, BSIP slide no. 15277, J35/4
31. *Lanagiopollis* sp. B, BSIP slide no. 15282, K45/4

Scale bar – 20 µm

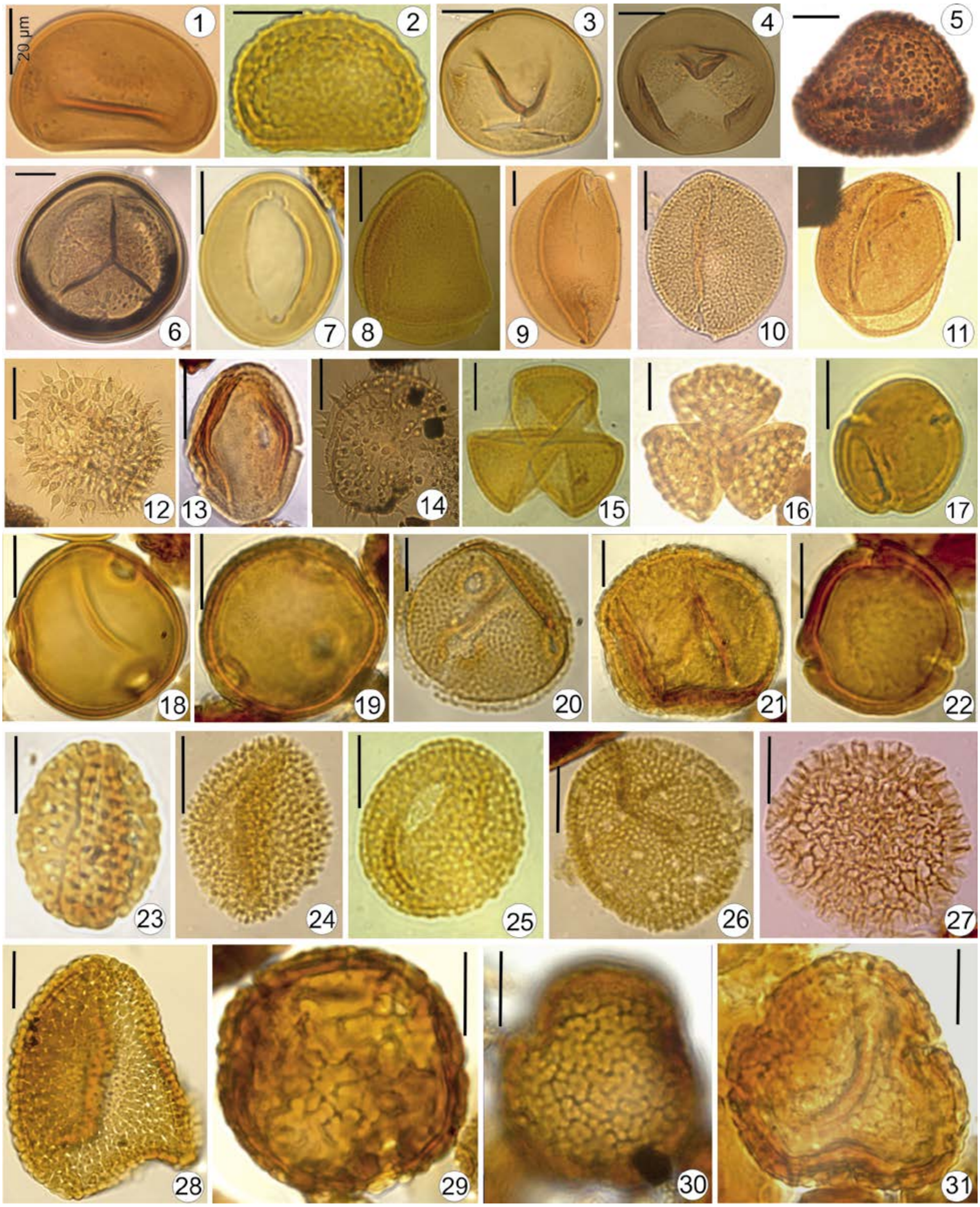
20 µm
1
2
3
4
5
6
7
8
9
10
11
12
13
14
15
16
17
18
19
20
21
22
23
24
25
26
27
28
29
30
31

Plate 2

1. *Verrumonosulcites* sp. Kar & Sharma, BSIP slide no. 1527, K31/1
2. *Clavaperporites heteroclavatus* Samant & Phadtare, BSIP slide no. 15289, N42/3
3. *Clavaperiporites homoclavatus* Samant & Phadtare, BSIP slide no. 15286 , P48
4. *Retipollenites enigmata* Venkatachala et al., BSIP slide no. 15288, G45/4
5. *Nyssapollenites incertus* Dutta & Sah, BSIP slide no. 15284, T39/3
6. *Arengapollenites ovatus* Samant & Phadtare, BSIP slide no. 15286, M47
7. Tetrad of *Arengapollenites ovatus* Samant & Phadtare, BSIP slide no. 15291, J21

8–9. Tetrad of *Arecipites wodehousei* Samant & Phadtare, BSIP slide no. 15289, R17

10. *Tribrevicolporites eocenicus* Kar, BSIP slide no. 15279, M23/3
11. *Mulleripollis bolpurensis* Baksi & Deb, BSIP slide no. 15277, J30
12. *Paripollis broachensis* Samant & Phadtare, BSIP slide no. 15277, P35
13. *Ctenolophonidites costatus* von Hoeken Klinkenberg, BSIP slide no. 15285, V49/3
14. *Retistephanocolpites brevicolpus* (Mathur) Saxena, BSIP slide no. 15285, T46/3
15. *Pseudonothophagidites kutchensis* Venkatachala & Kar, BSIP slide no. 15285, H29/3
16. *Diporisprites barrelis* Gupta, BSIP slide no. 15290, S26/4
17. *Callimothallus pertusus* Dilcher, BSIP slide no. 15303, M32
18. *Notothyrites setiferus* Cookson, BSIP slide no. 15297, U41/3
19. *Parmathyrites* sp., BSIP slide no. 15297, U33/2
20. Scoleodont teeth, BSIP slide no. 15300, F43
21. *Appendicisporites typicus* Saxena & Khare, BSIP slide no. 15298, G36/3
22. *Inapertisporites kedvesii* Elsik, BSIP slide no. 15285, S31/4
23. *Heliospermopsis* sp., BSIP slide no. 15308, Q29/3
24. *Phragmothyrites* sp., BSIP slide no. 15284, T48/3

25, 26, 29, 30. Planispiral microforaminiferal test linings, BSIP slide nos. 15303, T45, 15313, K42/4, 15312, Q48/4, 15314, K24/2

27–28. Trochospiral microforaminiferal test linings, BSIP slide nos. 15311, T28/4, 15299, J43

Scale bar – 20 µm

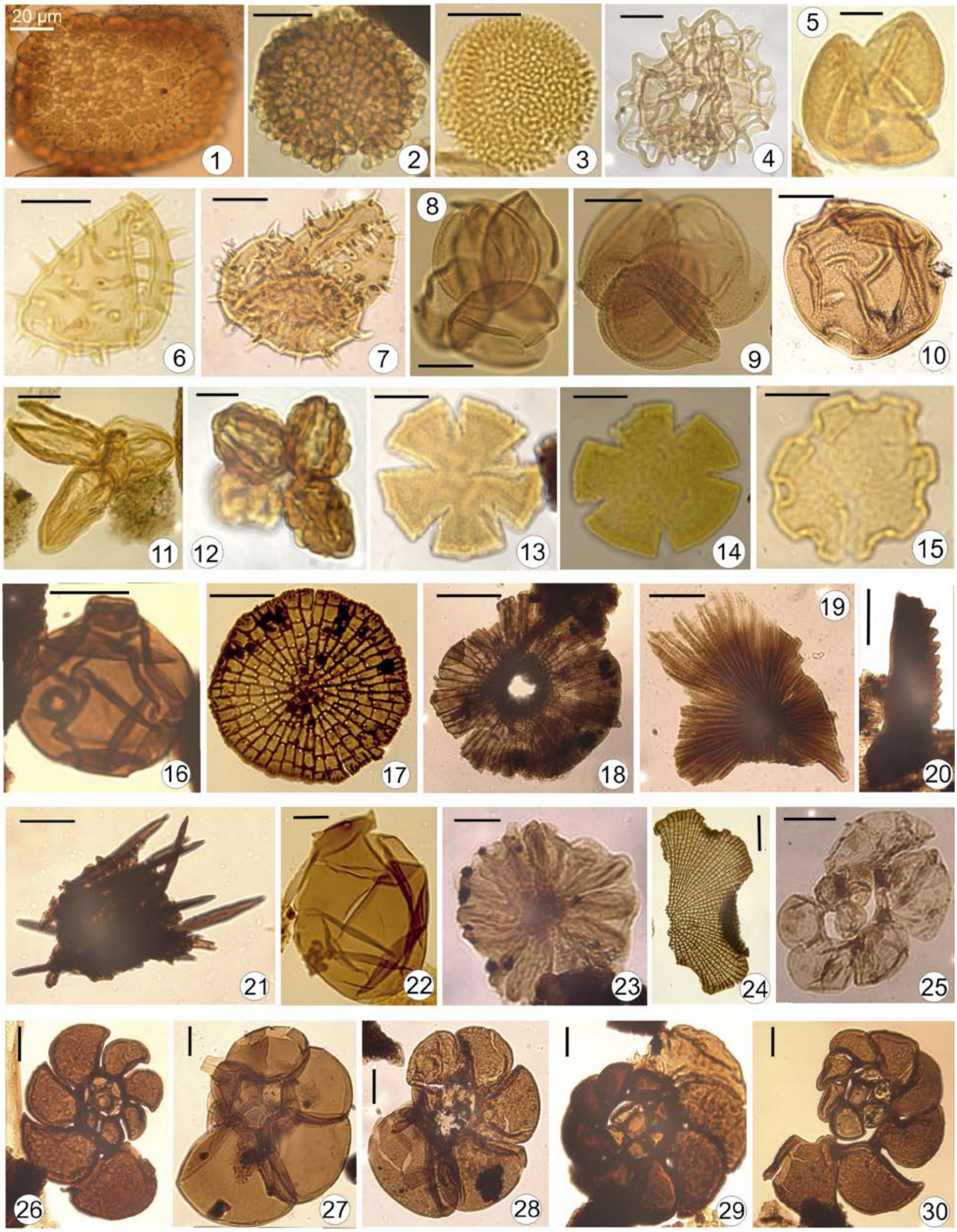
20 µm
1
2
3
4
5
6
7
8
9
10
11
12
13
14
15
16
17
18
19
20
21
22
23
24
25
26
27
28
29
30

Plate 3

1. *Botryococcus braunii* Kützing, BSIP slide no. 15277, L29

2, 7–10. *Operculodinium* sp., BSIP slide nos. 15305, L36, 15302, 15304, U38, 15304, 15306, G39/3, 15305, Q39/1

3. *Homotryblium tenuispinosum* Davey & Williams, BSIP slide no. 15303, T334- 6.

4–6. *Homotryblium abbreviatum* Eaton, BSIP slide nos. 15316, J30, 15295, U27/4, 15295, P46

11. *Cordosphaeridium fibrospinosum* Davey and Williams, BSIP slide no. 15316, O49/2

12. *Kenleyia* sp., BSIP slide no. 15301, M42/3

Scale bar – 20 µm

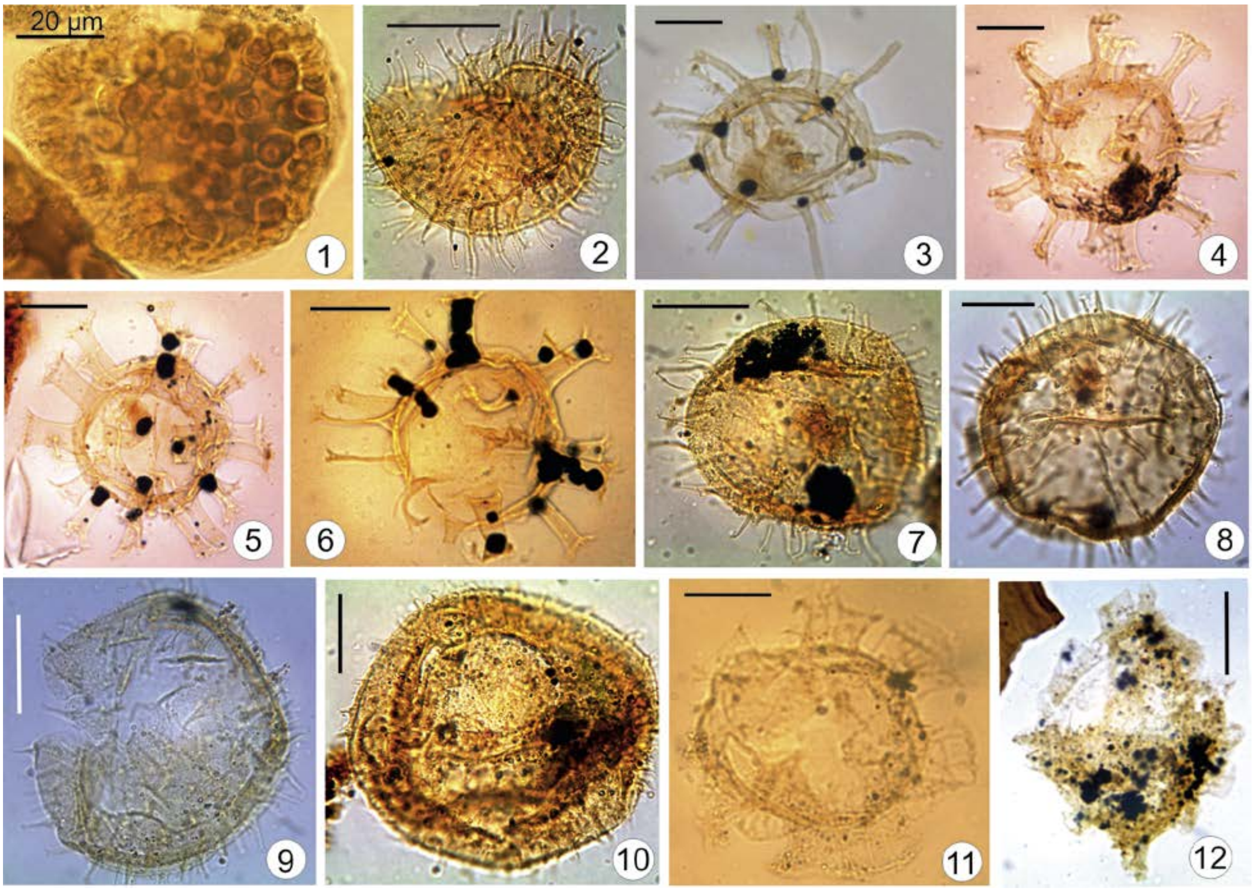
20 µm
1
2
3
4
5
6
7
8
9
10
11
12

Plate 4

1, 2, 4, 13. Leaf epidermal tissues, (1) showing stomata and accessory cells in normal transmitted light, (2) strong and (4) weak fluorescence under UV, (13) parenchymatous cells, BSIP slide nos. 15315, O39, 15301, K25/2

3, 9. Partially biodegraded leaf epidermal tissues, BSIP slide nos. 15293, O45/3, 15283

5. Biodegraded terrestrial organic matter, BSIP slide no. 15295, O45/4

6, 11. Amorphous organic matter under UV, showing (6) moderate and (11) weak fluorescence, BSIP slide no. 15294, Q22/4, K25/2

7, 8. Hyaline amorphous organic matter, (7) under normal transmitted light, (8) UV, BSIP slide nos. 15283, G43, 15294, T24/2

10, 14. Amorphous organic matter under normal transmitted light, BSIP slide nos. 15315, Q22

12, 15, 20. Resins, (12) under normal transmitted light, (15, 20) weak to moderate fluorescence under UV, BSIP slide nos. 15293, E 42/1, 15315, O40/3, 15243, O43/2.

16, 17. Hyaline vascular tissues, (16) under normal transmitted light, (17) non-fluorescing under UV, BSIP slide nos. 15293, N44, 15295, N45/4, T24/2

18. Biodegraded woody tissues under normal transmitted light, BSIP slide no. 15294

19. Black debris under UV, BSIP slide no. 15294, N45/4

Scale bar – 100 µm, or given on image

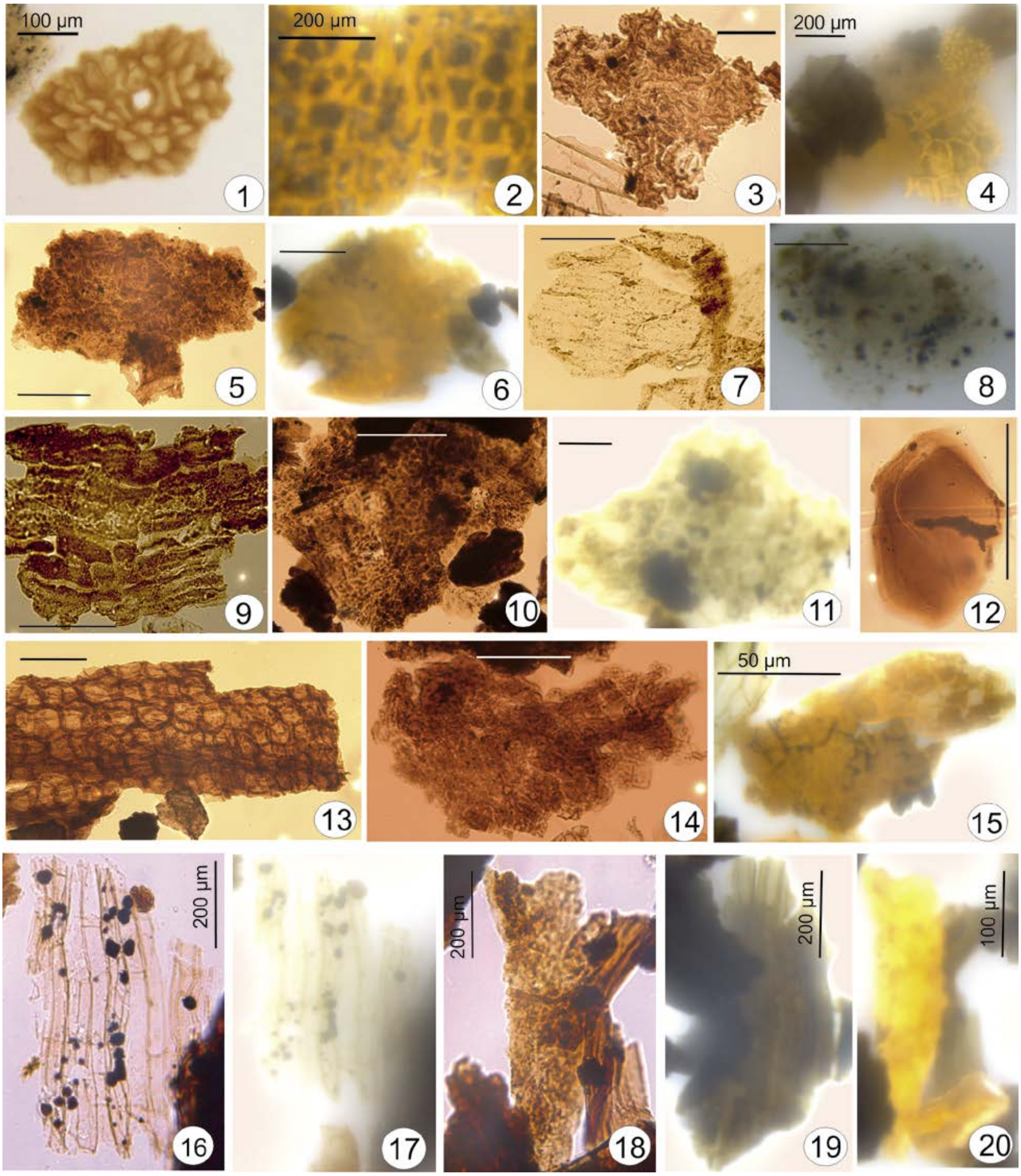
100 µm
200 µm
200 µm
50 µm
200 µm
200 µm
200 µm
100 µm
1
2
3
4
5
6
7
8
9
10
11
12
13
14
15
16
17
18
19
20